JACS
JOURNAL OF THE AMERICAN CHEMICAL SOCIETY

Communication

pubs.acs.org/JACS

Recombinant Sea Urchin Vascular Endothelial Growth Factor Directs Single-Crystal Growth and Branching in Vitro

Regina T. Knapp,[†] Ching-Hsuan Wu,[†] Kellen C. Mobilia, and Derk Joester*

Department of Materials Science and Engineering, Northwestern University, 2220 Campus Drive, Evanston, Illinois 60208, United States

Supporting Information

ABSTRACT: Biomineralization in sea urchin embryos is a crystal growth process that results in oriented single-crystalline spicules with a complex branching shape and smoothly curving surfaces. Uniquely, the primary mesenchyme cells (PMCs) that construct the endoskeleton can be cultured in vitro. However, in the absence of morphogenetic cues secreted by other cells in the embryo, spicules deposited in PMC culture lack the complex branching behavior observed in the embryo. Herein we demonstrate that recombinant sea urchin vascular endothelial growth factor (rVEGF), a signaling molecule that interacts with a cell-surface receptor, induces spiculogenesis and controls the spicule shape in PMC culture. Depending on the rVEGF concentration, PMCs deposit linear, "h"- and "H"-shaped, or triradiate spicules. Remarkably, the change from linear to triradiate occurs with a switch from bidirectional crystal growth parallel to the calcite *c* axis to growth along the three *a* axes. This finding has implications for our understanding of how cells integrate morphogenesis on the multi-micrometer scale with control over lattice orientation on the atomic scale. The PMC model system is uniquely suited to investigate this mechanism and develop biotechnological approaches to single-crystal growth.

Sea urchins make masterful use of intricately shaped single crystals in endoskeletal elements in all stages of their development.[1−4] For instance, the embryonic endoskeleton consists of two mirror-symmetric spicules composed of single-crystalline magnesian calcite ($Ca_{0.95}Mg_{0.05}CO_3$) and embedded proteins.[5] Primary mesenchyme cells (PMCs) deposit these spicules in a series of morphogenetic events. Key steps are an epithelial-to-mesenchyme transition, directional cell migration and patterning, and the formation of a syncytium by cell fusion (Figure 1a−e).[6,7] Spicule synthesis commences with the formation of a calcareous granule, which is elongated parallel to the crystallographic *a* axes into the triradiate rudiment. During further development, two of the radii change growth direction by 90° (from the *a* axes to the *c* axis). Further growth and additional branching events result in the mature endoskeleton (Figure 1f−j and Figure S1 in the Supporting Information). Spiculogenesis is carried out collaboratively and rapidly (5−13 μm h^{-1}) by the cells contributing to the syncytium[8] and has been shown to proceed through amorphous calcium carbonate (ACC) precursors.[9−11] Spicule growth occurs in a membrane-delimited privileged environment inside the cells.[12]

Remarkably, PMCs are autonomous in controlling the crystallography, connectivity, and decoration of the endoskeleton.[13] As a consequence, PMCs can be cultured in vitro and deposit single-crystalline spicules that resemble embryonic spicules.[5,14,15] This is the basis of our effort to micropattern cell-culture substrates for oriented growth of single crystals.[16] However, spicule growth in culture is predominantly bidirectional and parallel to the crystallographic *c* axis. In contrast, crystal growth in the embryo commences along the three *a* axes of a triradiate rudiment. Recently, ectoderm-derived homologs of vascular endothelial growth factor (VEGF) and fibroblast growth factor (FGF) were shown to play an integral role in PMC patterning and spicule formation.[17,18] While it is clear that the growth factors interact with their receptors located on the cell membrane, the outcomes and mechanisms of these signaling events remain poorly understood.

VEGF- and FGF-family proteins play an important role in directing cell migration and the formation and remodeling of vasculature and nervous networks.[19−22] Their role in branching morphogenesis led us to hypothesize that VEGF, beyond being a key "on" switch, might participate at two different levels of spiculogenesis: (i) controlling the gross geometry of growth, which is reflected by the first-formed embryonic triradiate spicule, and/or (ii) directing the crystal growth along specific directions. In this work, we investigated the effect of a recombinant sea urchin VEGF (rVEGF) on the shape and crystallography of spicules formed in *Strongylocentrotus purpuratus* PMC cultures.

We isolated the nucleotide sequence coding for a VEGF homolog from *Lytechinus pictus* using standard RT-PCR-based approaches. The corresponding protein LpVEGF (Figure S2) shows more than 80% sequence identity with its homologues in *Paracentrotus lividus* and *Hemicentrotus pulcherrimus*.[17,23] Sequence analysis revealed an N-terminal secretion signal peptide and a central cysteine knot. The cystine knot, a structural motif found in many other growth factors, consists of six cysteine residues forming three intramolecular disulfide bonds. Intermolecular dimerization by way of an additional disulfide bond is generally required for activation of the corresponding receptor.[24]

We generated a plasmid encoding a fusion protein comprising a C-terminal LpVEGF and an N-terminal maltose binding protein (MBP) for enhanced stability and solubility. To ensure

Received: September 18, 2012
Published: October 15, 2012

dx.doi.org/10.1021/ja309024b | *J. Am. Chem. Soc.* 2012, 134, 17908−17911

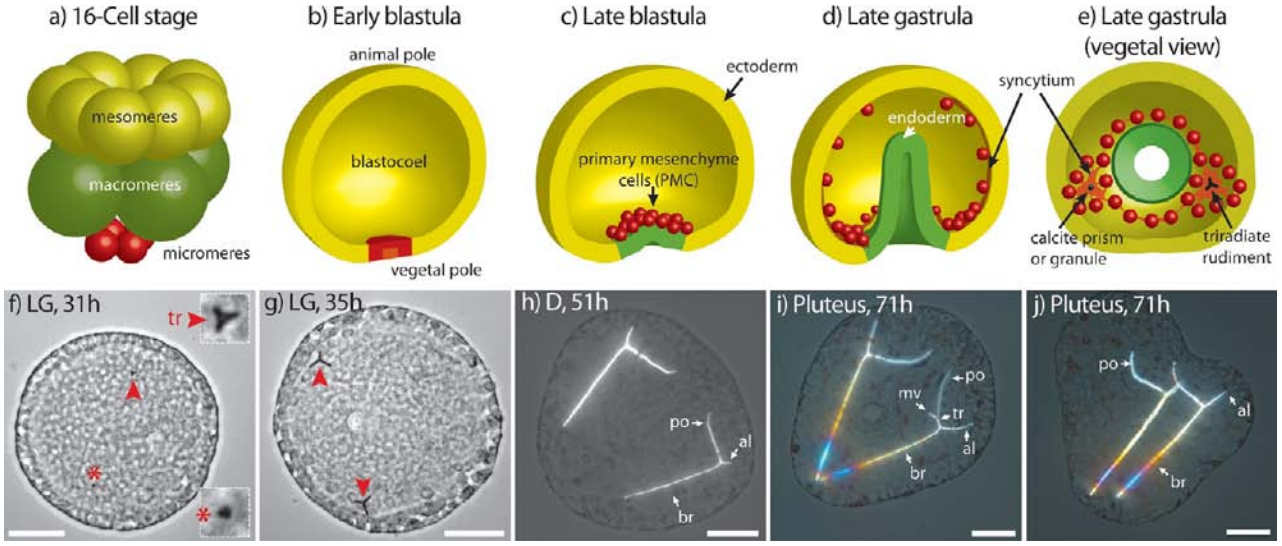

Figure 1. Early spiculogenesis in *S. purpuratus* embryos. (a, b) Micromeres formed in the fourth cleavage (a) congregate at the vegetal pole of the early blastula (b). (c) PMCs form and ingress during an epithelial-to-mesenchymal transition that is completed by the late blastula/early gastrula stage. (d, e) In the gastrula stage, PMCs migrate and fuse to form two mirror-symmetric syncytial masses. A calcite granule or prism is first deposited in each syncytium (marked by the asterisk in f). (f, g) Growth parallel to the *a* axes leads to the triradiate rudiment (tr) (marked by arrowheads). One of the radii continues growing along the *a* direction, and another bends by 90° to form the body rod (br). The third radius remains the short midventral rod (mv). (h–j) At the transition from prism (Δ) to pluteus [(i) top view, (j) oblique side view], the postoral rod (po) changes growth direction and the anterolateral rod (al) branches from the body rod. Scale bars represent 50 μm.

Table 1. Dependence of Spicule Density on rVEGF Concentration

HS (%)	FBS (%)	rVEGF lysate (μg mL^{-1})[a]	MBP lysate (μg mL^{-1})[a]	spicule number density[b]
–	4.0	–	–	6 ± 4[c]
–	4.0	0.5	–	5 ± 3[d]
–	4.0	1.0	–	14 ± 4[d]
–	4.0	2.5	–	46 ± 6[d]
–	4.0	–	2.5	2 ± 1[e]
4.0	–	–	–	17 ± 10[d]

[a]Total protein content in the lysate as determined by bicinchoninic acid (BCA) assay. [b]Average number of spicules per frame (0.60 mm^2) in *N* microscope image frames. Images were taken at ≥96 h post fertilization (hpf). [c]*N* = 3. [d]*N* = 6. [e]*N* = 5.

proper disulfide bond formation, the fusion protein was expressed in an *Escherichia coli* strain (SHuffle Express, New England BioLabs) that produces cytosolic disulfide bond isomerase C. For the following experiments, lysates of bacteria expressing the fusion protein are called rVEGF, and lysates of bacteria expressing a construct coding for MBP but lacking LpVEGF are called MBP (Figure S3).

PMCs in culture are commonly induced to form spicules by supplying 4% horse serum (HS) in the medium.[14] While it is not clear which factors are responsible for induction, it is likely that they simulate VEGF and possibly other factors present in the embryo. In the presence of fetal bovine serum (FBS), the number density of spicules is greatly reduced. We consequently used FBS-supplemented media to investigate the effect of rVEGF on spiculogenesis.

A clear dose-dependent effect of rVEGF on the number density of linear spicules formed was found (Table 1). An rVEGF concentration of 1 μg mL^{-1} was sufficient to increase spicule formation by a factor of >2 over the background, approximately equal to the effect of 4% HS. The spicule number density was directly proportional to the rVEGF concentration up to 2.5 μg mL^{-1}. MBP did not induce spiculogenesis above background (Figure S4). We conclude that the recombinant MBP–VEGF is functionally active. As the formation of syncytia and the deposition of calcareous granules by PMCs do not depend on external factors,[14] VEGF appears to control spicule elongation (i.e., crystal growth rather than nucleation).

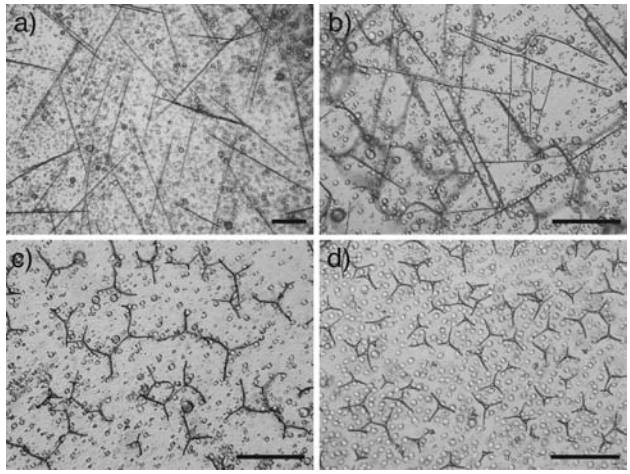

Figure 2. Morphogenetic effect of rVEGF. (a–d) *S. purpuratus* PMCs treated with increasing concentrations of rVEGF deposit (a) linear spicules at 5 μg mL^{-1}, (b) "h"- and "H"-shaped spicules at 15 μg mL^{-1}, (c) large triradiates at 30 μg mL^{-1}, and (d) small triradiates at 120 μg mL^{-1}. Images were taken at 96 hpf. Scale bars represent 100 μm.

Indeed, treatment of *S. purpuratus* PMC cultures with increasing concentrations of rVEGF had dramatic consequences on the spicule shape (Figure 2 and Figure S5). At ≤5 μg mL^{-1}, the spicules were predominantly linear rods with a small number of bifurcated spicules resembling tuning forks (Figures 2a and S5a). At intermediate concentrations, "h"- and "H"-shaped spicules were observed (Figures 2b and S5b). At ≥30 μg mL^{-1}, triradiate spicules that closely resembled the triradiate rudiments

dx.doi.org/10.1021/ja309024b | *J. Am. Chem. Soc.* 2012, 134, 17908–17911

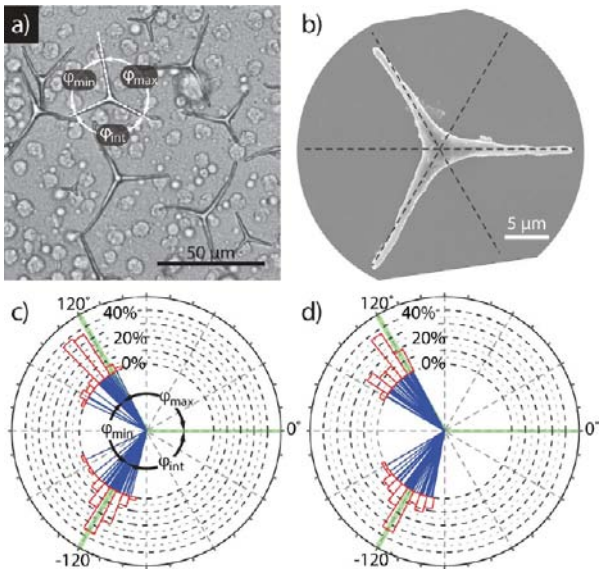

Figure 3. Histograms of triradiate angles. (a) Typical light microscopy image of triradiate spicules. The scale bar represents 50 μm. (b) Scanning electron microscopy (SEM) image of a triradiate after removal of cellular material, revealing smooth surfaces. Even though the branching angles were a nearly perfect 120° close to the branch point, at distances of >7 μm the radii were slightly bent away from their original direction. The scale bar represents 5 μm. (c, d) Angular histograms of triradiates grown at (c) 30 μg mL^{-1} rVEGF (N = 50) and (d) 120 μg mL^{-1} rVEGF (N = 50), showing that there was usually one angle slightly larger and one slightly smaller than 120°.

in the sea urchin embryo were deposited (Figures 2c,d and S5c,d).

Remarkably, triradiates in vitro grew past their typical size in embryos (up to 40 μm radius vs 3−5 μm in the embryo) (Figure 2c,d) and did not branch further. One of the angles between the radii was frequently close to 120°, one was smaller, and one was larger (Figure 3c,d). However, the center of the triradiate usually had close to perfect threefold symmetry. It appears that the radii gradually changed direction once they became larger than 3−5 μm.

In polarized light, the linear and h/H-shaped spicules behaved as single crystals elongated along the calcite c axis (Figure S5a,b). The spicules brightened when the long axis was oriented at an angle of 45° and were extinguished as a whole at 0 and 90° (Figure S6). In contrast, most of the triradiate spicules were extinguished at all angles (Figure S5c,d), indicating that the axis of birefringence (i.e., the calcite c axis) was parallel to the optical axis of the microscope and the radii were in the (001) plane.

To confirm this assessment, cleaned spicules were used as a substrate for epitaxial overgrowth with calcite by exposure to a supersaturated solution. Newly deposited crystals displayed the typical rhombohedral calcite habit with facets corresponding to the {104} planes (Figure 4). For linear, h/H-shaped, and triradiate spicules, the facets were consistently parallel over the body of the entire spicule, confirming their single-crystalline nature.

The orientation of the calcite lattice was determined from the characteristic angles at the vertices of the rhombohedra. For linear spicules deposited at low concentrations of rVEGF, the long axis of the spicule was parallel to the calcite c axis (Figure 4a,b), similar to those grown in the presence of HS.[16] For h/H-shaped spicules, the rods corresponding to the vertical strokes were oriented parallel to the c axis. The horizontal crossbar was close to one of the a axes in the plane (Figure 4c,d). Triradiate spicules displayed radii that coincided with the a axes close to the branch point (Figure 4e,f), identical to the triradiate rudiments in sea urchin embryos.[25]

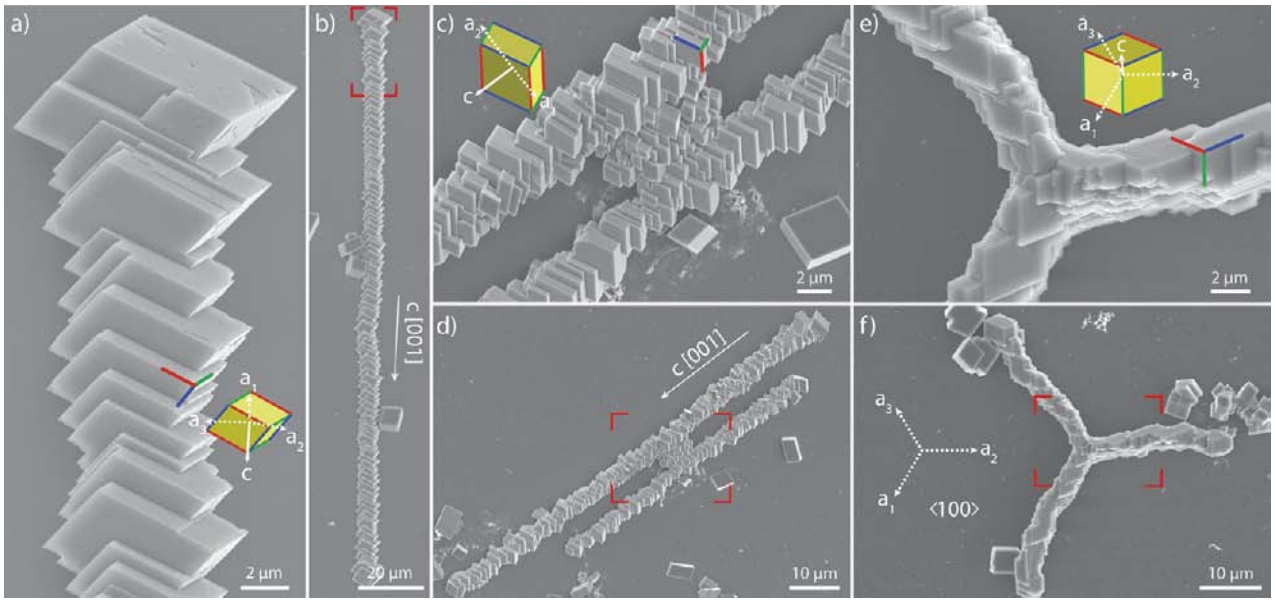

Figure 4. Influence of rVEGF on the crystal growth direction. (a, b) Epitaxial overgrowth of spicules after removal of organic matter revealed that linear spicules were elongated parallel to the c axis. (c, d) In h/H-shaped spicules, the crossbar was in the (001) plane and frequently close to one of the a directions. The elements corresponding to the vertical strokes of the "h" or "H" were parallel to the c axis. (e, f) Triradiate spicules showed branching in the (001) plane, parallel to the three a axes. Rendered {104} rhombohedra (yellow) indicate the calcite lattice orientation inferred from the projected angles between the edges (red, green, and blue lines). The rectangle vertices marked in red in (b, d, f) indicate the locations of details shown in the corresponding panels (a, c, e).

dx.doi.org/10.1021/ja309024b | J. Am. Chem. Soc. 2012, 134, 17908−17911

We conclude that the VEGF concentration controls both the gross morphology and the single-crystal branching along defined crystallographic directions. At low rVEGF concentration, the default growth direction is along the positive and negative calcite *c* axis. At intermediate concentrations, there could be a brief initial phase where growth occurs along one *a* axis only, followed by growth along the default *c* axis. This change in growth direction would lead to h-shaped spicules. Occasionally, the switch from the *a* direction to the *c* direction leads to two new branches growing in opposite directions, resulting in the H-shaped spicules. Further increasing the rVEGF concentration stabilizes growth along all three *a* axes and gives rise to triradiate spicules. This requires a mechanism by which PMCs sense the orientation of the calcite lattice and adjust the direction of spicule elongation accordingly. However, we observed that directional control gradually weakens with increasing distance from the branch site. This could be a consequence of the inability of the cells to exert strict control over the relative positioning of the spicule elongation sites at larger distances or indicate that ACC deposited during spicule growth interferes with sensing of the lattice direction.[9,11]

In summary, VEGF in the sea urchin embryo acts as a molecular switch that controls the elongation of a single crystal along specific crystallographic directions inside the PMC syncytium. As a signaling molecule, VEGF interacts with cell-surface receptors but not with the forming mineral. In the embryo, where the VEGF concentration to which PMCs are exposed very likely depends on the distance to the VEGF-expressing ectodermal cells and time, this mechanism may be responsible for a significant part of the morphogenetic events during early spiculogenesis. Additional factors may be required for control of further branching events during later stages. The concentration-dependent branching may well share elements of the VEGF/FGF-dependent regulatory networks that govern branching morphogenesis in other systems. While there are a few examples of specific proteins involved in polymorph control, such as Starmaker in the zebrafish otolith,[26] N16,[27] and Pif in the pearl oyster,[28] our understanding of the biological regulation of biomineral morphosynthesis is still very limited. PMC culture presents a unique opportunity to investigate the entire chain of events at the transcriptome, proteome, and ultrastructural levels. Unraveling the mechanism by which PMCs sense an atomic-scale property (lattice orientation) and use this information to elongate the single crystal in a specific direction may now be within reach.

■ ASSOCIATED CONTENT

Ⓢ Supporting Information

Experimental procedures, construction of rVEGF, cell culture, optical microscopy, and SEM. This material is available free of charge via the Internet at http://pubs.acs.org.

■ AUTHOR INFORMATION

Corresponding Author

d-joester@northwestern.edu

Author Contributions

†These authors contributed equally.

Notes

The authors declare no competing financial interest.

■ ACKNOWLEDGMENTS

This work was supported in part by the U.S. National Science Foundation (NSF) (DMR-0805313 and DMR-1106208), the NSF MRSEC Program (DMR-1121262) at the Materials Research Center of Northwestern University (NU), and the International Institute for Nanotechnology at Northwestern University. We thank Fred Wilt for stimulating discussion. Gel imaging and UV/vis spectrophotometry were performed at the NU Keck Biophysics Facility, an NU core facility supported by a Cancer Center Support Grant (NCI CA060553). SEM was performed at NUANCE, an NU core facility supported by NSF-NSEC, NSF-MRSEC, the Keck Foundation, the State of Illinois, and NU. Traditional sequencing services were performed at the NU Genomics Core Facility. We thank E. Campbell, A. Park, L. Mueller, and F. Y. Luk for technical assistance.

■ REFERENCES

(1) Lowenstam, H. A.; Weiner, S. *On Biomineralization*; Oxford University Press: New York, 1989.

(2) Ma, Y. R.; Aichmayer, B.; Paris, O.; Fratzl, P.; Meibom, A.; Metzler, R. A.; Politi, Y.; Addadi, L.; Gilbert, P.; Weiner, S. *Proc. Natl. Acad. Sci. U.S.A.* **2009**, *106*, 6048.

(3) Dubois, P.; Ameye, L. *Microsc. Res. Technol.* **2001**, *55*, 427.

(4) Matranga, V.; Bonaventura, R.; Costa, C.; Karakostis, K.; Pinsino, A.; Russo, R.; Zito, F. *Prog. Mol. Subcell. Biol.* **2011**, *52*, 225.

(5) Killian, C. E.; Wilt, F. H. *Chem. Rev.* **2008**, *108*, 4463.

(6) Ettensohn, C. A. *Development* **2009**, *136*, 11.

(7) Lyons, D. C.; Kaltenbach, S. L.; McClay, D. R. *Wiley Interdiscip. Rev.: Dev. Biol.* **2012**, *1*, 231.

(8) Guss, K. A.; Ettensohn, C. A. *Development* **1997**, *124*, 1899.

(9) Gong, Y. U. T.; Killian, C. E.; Olson, I. C.; Appathurai, N. P.; Amasino, A. L.; Mantin, M. C.; Holt, L. J.; Wilt, F. H.; Gilbert., P. U. P. A. *Proc. Natl. Acad. Sci. U.S.A.* **2012**, *109*, 2088.

(10) Politi, Y.; Levi-Kalisman, Y.; Raz, S.; Wilt, F.; Addadi, L.; Weiner, S.; Sagi, I. *Adv. Funct. Mater.* **2006**, *16*, 1289.

(11) Politi, Y.; Metzler, R. A.; Abrecht, M.; Gilbert, B.; Wilt, F. H.; Sagi, I.; Addadi, L.; Weiner, S.; Gilbert, P. *Proc. Natl. Acad. Sci. U.S.A.* **2008**, *105*, 17362.

(12) Beniash, E.; Addadi, L.; Weiner, S. *J. Struct. Biol.* **1999**, *125*, 50.

(13) Armstrong, N.; McClay, D. R. *Dev. Biol.* **1994**, *162*, 329.

(14) Okazaki, K. *Am. Zool.* **1975**, *15*, 567.

(15) Wilt, F. H.; Benson, S. C. In *Development of Sea Urchins, Ascidians, and Other Invertebrate Deuterostomes: Experimental Approaches*; Academic Press: San Diego, 2004; Vol. *74*, p 273.

(16) Wu, C.-H.; Park, A.; Joester, D. *J. Am. Chem. Soc.* **2011**, *33*, 1658.

(17) Duloquin, L.; Lhomond, G.; Gache, C. *Development* **2007**, *134*, 2293.

(18) Röttinger, E.; Saudemont, A.; Duboc, V.; Besnardeau, L.; McClay, D.; Lepage, T. *Development* **2008**, *135*, 353.

(19) Ferrara, N.; Gerber, H. P.; LeCouter, J. *Nat. Med.* **2003**, *9*, 669.

(20) Luo, J.; Xiong, Y.; Han, X.; Lu, Y. *J. Mol. Med.* **2011**, *89*, 635.

(21) Adams, R. H.; Eichmann, A. *Cold Spring Harbor Perspect. Biol.* **2010**, *2*, No. a001875.

(22) Cho, N. K.; Keyes, L.; Johnson, E.; Heller, J.; Ryner, L.; Karim, F.; Krasnow, M. A. *Cell* **2002**, *108*, 865.

(23) Fujita, K.; Takechi, E.; Sakamoto, N.; Sumiyoshi, N.; Izumi, S.; Miyamoto, T.; Matsuura, S.; Tsurugaya, T.; Akasaka, K.; Yamamoto, T. *Mech. Dev.* **2010**, *127*, 235.

(24) Sun, P. D.; Davies, D. R. *Annu. Rev. Biophys. Biomol. Struct.* **1995**, *24*, 269.

(25) Okazaki, K.; Inoue, S. *Dev., Growth Differ.* **1976**, *18*, 413.

(26) Sollner, C.; Burghammer, M.; Busch-Nentwich, E.; Berger, J.; Schwarz, H.; Riekel, C.; Nicolson, T. *Science* **2003**, *302*, 282.

(27) Samata, T.; Hayashi, N.; Kono, M.; Hasegawa, K.; Horita, C.; Akera, S. *FEBS Lett.* **1999**, *462*, 225.

(28) Suzuki, M.; Saruwatari, K.; Kogure, T.; Yamamoto, Y.; Nishimura, T.; Kato, T.; Nagasawa, H. *Science* **2009**, *325*, 1388.